Fail-Safe Spacecraft Rendezvous on Near-Rectilinear Halo Orbits

Aguilar Marsillach, Daniel; Di Cairano, Stefano; Kalabic, Uros; Weiss, Avishai

TR2021-054 June 04, 2021

Abstract

Future spacecraft missions require novel guidance and control policies that reduce fuel consumption, yield sparse thrust signals, and maintain mission safety even in the presence of faults. This paper presents an approach for rendezvous with a target in a near-rectilinear halo orbit that exploits the natural dynamics to reduce propellant consumption, and ensures passive safety in the presence of thruster failure. A chaser spacecraft that aims to rendezvous with a target is steered into coasting sets while simultaneously maintaining passive safety by avoiding the states that naturally collide with the target. Upon entering the coasting sets, the chaser's thrusters are disengaged, as the natural dynamics lead it into a goal set. Abort-safety is then demonstrated during final approach from the goal set to the target. The target is modeled in a full-ephemeris, high-fidelity, and quasi-periodic near-rectilinear halo orbit. Simulations demonstrate a reduction in maneuver fuel consumption, measured by delta-v, of up to 72.5% and a significant reduction of thruster on-time compared to prior work.

American Control Conference (ACC) 2021

Fail-Safe Spacecraft Rendezvous on Near-Rectilinear Halo Orbits

Daniel Aguilar Marsillach[1], Stefano Di Cairano[2], Uroš Kalabić[3], Avishai Weiss[4]

***Abstract*— Future spacecraft missions require novel guidance and control policies that reduce fuel consumption, yield sparse thrust signals, and maintain mission safety even in the presence of faults. This paper presents an approach for rendezvous with a target in a near-rectilinear halo orbit that exploits the natural dynamics to reduce propellant consumption, and ensures passive safety in the presence of thruster failure. A chaser spacecraft that aims to rendezvous with a target is steered into coasting sets while simultaneously maintaining passive safety by avoiding the states that naturally collide with the target. Upon entering the coasting sets, the chaser's thrusters are disengaged, as the natural dynamics lead it into a goal set. Abort-safety is then demonstrated during final approach from the goal set to the target. The target is modeled in a full-ephemeris, high-fidelity, and quasi-periodic near-rectilinear halo orbit. Simulations demonstrate a reduction in maneuver fuel consumption, measured by delta-v, of up to 72.5% and a significant reduction of thruster on-time compared to prior work.**

I. INTRODUCTION

Improved online trajectory generation and control is necessary for increased spacecraft autonomy in increasingly complex mission scenarios [1]. Motivated by NASA's Lunar Orbital Platform-Gateway concept [2], this work considers rendezvous with a target body in a high fidelity quasi-periodic near-rectilinear halo orbit (NRHO). During rendezvous, the approaching vehicle must avoid collision with the target, even under thruster failure. Initially, the approaching spacecraft, called the chaser, must remain passively-safe with respect to the target for a pre-defined time duration [3]. That is, free-drift trajectories along its approach do not enter an avoidance region around the target. Upon closer proximity to the target, abort-safety must be maintained such that in the event of a partial loss of control, the chaser is able to perform a powered-abort maneuver to avoid colliding with the target [3]–[5].

Fail-safe spacecraft rendezvous can be cast as a trajectory generation and control problem that avoids unsafe regions of state space in which collision is guaranteed under total or partial thrust failure. The unsafe regions can be characterized using reachability theory [5]–[7]. Additionally, spacecraft missions often seek to minimize delta-v, which provides a measure of the total propellant consumed throughout a maneuver [8]. When introducing non-convex safety constraints, it becomes difficult to solve for the optimal delta-v maneuver in a computationally efficient manner [9]. As such, the non-convex constraints are often locally approximated as convex constraints, yielding a feasible sub-optimal solution that remains fuel efficient. These convexified constraints have been exploited to maintain passive safety using MPC [4], [5], [10], [11]. Moreover, thruster on-time may be reduced by incorporating thruster on-off integer decision variables in the optimization [12]. Combining safety and thruster on-off decision variables requires solving a non-convex mixed-integer program, which is challenging for on-board implementation. Thus, a computationally tractable approach that satisfies the safety constraints while improving performance in terms of delta-v and reduced thruster on-time is desirable.

We propose a solution to this problem by leveraging natural orbital dynamics using passive backwards reachable sets (PBRS). The resulting methodology allows the chaser to enter a coasting-arc where no control is required to safely coast toward a goal region of interest. This expands on our prior work on passive and abort-safe spacecraft rendezvous about time-varying reference trajectories [5], [11] by improving delta-v performance and reducing thruster usage through coasting-arcs. The results in this paper focus on a rendezvous mission concept for a target in an NRHO. Prior work for NRHO rendezvous has considered the design of safe approach trajectories in an offline manner [13], [14]. These works however do not consider safety with respect to general failure modes.

The target NRHO used in this work is constructed using a full ephemeris model and dominant perturbations [15]. The equations of motion of the target in the resulting near-stable quasi-periodic orbit are linearized, resulting in a linear-time varying (LTV) system from which the PBRS, passive-unsafe, and abort-unsafe sets are computed. Initially, when far from the target, passive-safety is maintained and coasting arcs are exploited. Once the chaser enters a final approach corridor given by a line-of-sight (LOS) cone, abort-safety with respect to an assumed failure mode is considered.

A. Preliminaries and Notation

Vectors are shown in boldface. $\mathbb{R}^n$ denotes the n-dimensional Euclidean space. I_n denotes the n-dimensional identity matrix. We denote the value of a signal at a discrete time k as $\boldsymbol{x}_k$, and $\boldsymbol{x}_{k|t}$ denotes the value of $\boldsymbol{x}$ predicted k steps ahead from t. The complement of a set $\mathcal{X}$ is given by $\mathcal{X}^{\mathrm{c}}$. The hyperplane representation of the polyhedron $\mathcal{P} \subseteq \mathbb{R}^n$ is $\mathcal{P}(H, \boldsymbol{k}) = \{\boldsymbol{x} \in \mathbb{R}^n : \ H\boldsymbol{x} \leq \boldsymbol{k}\}$ with $H \in \mathbb{R}^{p \times n}$, $\boldsymbol{k} \in \mathbb{R}^p$. An ellipsoid centered at $\mathbf{d} \in \mathbb{R}^n$ with shape matrix D, is $\mathcal{E}(\mathbf{d}, D) \triangleq \{\mathbf{x} \in \mathbb{R}^n \ : \ (\mathbf{x}-\mathbf{d})^\top D^{-1}(\mathbf{x}-\mathbf{d}) \leq 1\}$. Given a matrix H, $[H]_i$ denotes the i^{th} row of the matrix.

[1] D. Aguilar Marsillach is with the Department of Aerospace Engineering Sciences at the University of Colorado - Boulder, Boulder, CO 80303, USA. Email: d.aguilar@colorado.edu. He interned at MERL during the development of this work.

[2,3,4] S. Di Cairano, U. Kalabić, and A. Weiss are with Mitsubishi Electric Research Laboratories, Cambridge, MA 02139, USA. Emails: {dicairano,kalabic,weiss}@merl.com

II. Spacecraft Model

Consider a target and a chaser in orbit around two primary bodies, e.g. Earth and the Moon. The spacecraft are assumed to be rigid bodies such that all exogenous forces act on their centers of mass and the target spacecraft is assumed to be uncontrolled.

A. Translational Dynamics

The dynamics of the chaser relative to the target are obtained by considering the Earth and Moon's gravitational forces and dominant perturbations [14], [15].

Since linearized dynamics dominate around some nominal trajectory, we can describe the relative motion of a chaser with respect to the target by linearizing the nonlinear dynamics about the target's nominal trajectory $\boldsymbol{x}_n(t)$. The variation $\delta\boldsymbol{x} = \boldsymbol{x}_\mathrm{c} - \boldsymbol{x}_n$, provides the relative state of the chaser with respect to the target's nominal trajectory. We define $\boldsymbol{x} \triangleq \delta\boldsymbol{x}$, and $\boldsymbol{u}$ as the chaser's control input. In this work we consider a discrete time formulation of the continuous LTV equations with sampling period Δt, which is assumed to be small enough not to lose significant behavior between samples, yielding

$$\boldsymbol{x}_{t+1} = \boldsymbol{f}(t, \boldsymbol{x}_t, \boldsymbol{u}_t) = A_d(t)\boldsymbol{x}_t + B_d(t)\boldsymbol{u}_t. \tag{1}$$

B. Thruster Configuration

As shown in [5], for given a thruster configuration, we can construct a general polytopic and compact admissible control set

$$\mathcal{U} = \{\boldsymbol{u} \in \mathbb{R}^3 : H_u\boldsymbol{u} \le \boldsymbol{k}_u\}, \tag{2}$$

where $\mathbf{0} \in \mathcal{U}$. For simplicity, in this work the control vector is constrained only by lower and upper bounds, $\boldsymbol{u}_l$ and $\boldsymbol{u}_u$, respectively. Hence, $\boldsymbol{k}_u$ in (2) is completely determined by $\boldsymbol{u}_l$ and $\boldsymbol{u}_u$. Let $\boldsymbol{k}_{u,i}$ correspond to the admissible control set $\mathcal{U}_i$. For accounting for safety with respect to partial or total loss of thrust, it is sufficient to consider distinct $\boldsymbol{k}_{u,i}$ for the different failure modes. The set of possible failure modes, $\mathcal{FM}$ is therefore given by $\mathcal{FM} = \{\boldsymbol{k}_{u,1}, \ldots, \boldsymbol{k}_{u,n_\mathrm{F}}\}$, where $n_\mathrm{F} = |\mathcal{FM}|$ is the total number of failure modes under consideration. We let $\mathcal{U}_i$ denote the admissible control set corresponding to failure mode $\mathcal{FM}_i \in \mathcal{FM}$. These failure modes are used to construct the set of states for which all control actions lead to collision with a polytopic terminal set [5].

III. Reachable Sets and Safety

The RBRS is the set of all states for which the terminal set is entered regardless of the control actions. Thus, if a failure were to occur when the state is in the complement of the RBRS, then there exists an admissible abort sequence such that the chaser avoids colliding with the target. The PBRS is a special case of the RBRS where the system evolves only according the natural dynamics, i.e., $\mathcal{U} = \{\mathbf{0}\}$. Additional details on PBRS and RBRS for passive and abort safety are in [5], [11].

Definition III.1. *Given $\boldsymbol{x}_{t+1} = \boldsymbol{f}(t, \boldsymbol{x}_t, \boldsymbol{u}_t)$, a convex admissible control set $\mathcal{U}$ where $\boldsymbol{u} \in \mathcal{U}$, and final time t_f, the N-steps robust backward reachable set $\mathcal{R}_b(N; \mathcal{S}_f, \mathcal{U}, t_f)$ of target region $\mathcal{S}_f \subseteq \mathbb{R}^n$ is*

$$\begin{aligned}
&\mathcal{R}_b(0; \mathcal{S}_f, \mathcal{U}, t_f) = \mathcal{S}_f, \\
&\mathcal{R}_b(j; \mathcal{S}_f, \mathcal{U}, t_f) = \{\boldsymbol{x} \in \mathbb{R}^n : \\
&\qquad \boldsymbol{f}(t_f - j\Delta t, \boldsymbol{x}, \boldsymbol{u}) \in \mathcal{R}_b(j-1; \mathcal{S}_f, \mathcal{U}, t_f), \forall \boldsymbol{u} \in \mathcal{U}\}, \\
&\qquad j \in \{1, \ldots, N\}.
\end{aligned} \tag{3}$$

The RBRS is the set of states at time $t_j = t_f - j\Delta t$ from which the chaser will not be able to avoid collision at time t_f, regardless of the admissible control sequence applied.

Definition III.2. *The robust backwards reachable set over the time interval $[t_0, t_f]$ (RBRSI), where $t_0 = t_f - N\Delta t$, is the union of the j-steps RBRS,*

$$\mathcal{R}(N; \mathcal{S}_f, \mathcal{U}, t_f) = \bigcup_{j=0}^{N} \mathcal{R}_b(j; \mathcal{S}_f, \mathcal{U}, t_f). \tag{4}$$

The RBRSI denotes the set of states $\bar{\boldsymbol{x}}$ for which there exists $t \in [t_0, t_f]$, such that from $\boldsymbol{x}(t) = \bar{\boldsymbol{x}}$, the chaser will not be able to avoid collision at time t_f, no matter the admissible control sequence applied.

Next, we account for changing final time since the target orbit is not periodic. To this end the LTV-RBRSI is the union of various RBRSI over $[t_0, t_f]$, with $t_f - t_0 = N\Delta t$

$$\bar{\mathcal{R}}(N; \mathcal{S}_f, \mathcal{U}) = \bigcup_{j=0}^{N} \mathcal{R}(j; \mathcal{S}_f, \mathcal{U}, t_0 + j\Delta t), \tag{5}$$

which provides the union for increasing final times so that safety is maintained with respect to the LTV system. Therefore, $N\Delta t$ uniquely defines the safety-horizon duration under consideration.

To be safe with respect to various failure modes, the union of the LTV-RBRSI has to be taken over various input sets. The *unsafe sets* are constructed from $q \le n_F$ input sets as

$$\bar{\mathcal{R}}_\mathrm{unsafe}(N; \mathcal{S}_f) = \bigcup_{i=1}^{q} \bar{\mathcal{R}}(N; \mathcal{S}_f, \mathcal{U}_i). \tag{6}$$

In (6), it is enough to consider all input sets that are not supersets of others, i.e., $\{\mathcal{U}_i : i, j \in \{1, \ldots q\}, \nexists j \le i, \mathcal{U}_i \supseteq \mathcal{U}_j\}$, so that we can ignore the input set for nominal conditions. Hence the safe set with respect to q failure modes is given by

$$\mathcal{X}_\mathrm{safe}^{N,q} = \bar{\mathcal{R}}_\mathrm{unsafe}(N; \mathcal{S}_f)^\mathrm{c}. \tag{7}$$

The above expressions for unsafe sets are general and rely only on compactness of the terminal set. In this work, we further require that the terminal set be polytopic or ellipsoidal, which is not a significant restriction, and which significantly improves the speed of computation of unsafe sets and leads to a more efficient representation of constraints.

A. Polytopic Robust Backwards Reachable Sets

When the dynamics are linear and the target set $\mathcal{S}_f$ is a polytope, the RBRS is also a polytope and is computed by solving linear programs [6]. Hence the unsafe set is a union of polytopes that are computed to take into account the LTV nature of the equations of relative motion as well as well as the different admissible control sets associated to the possible failure modes. Consider the target set $\mathcal{P}_f = \mathcal{P}(H_f, \boldsymbol{k}_f)$. Let the j-steps RBRS from final time t_f be $\mathcal{R}_b(j; \mathcal{P}_f, \mathcal{U}, t_f) = \mathcal{P}(H_j, \boldsymbol{k}_j)$, the $j+1$-steps RBRS is $\mathcal{R}_b(j+1; \mathcal{P}_f, \mathcal{U}, t_f) = \{\boldsymbol{x} \in \mathbb{R}^n : \ H_{j+1}\boldsymbol{x} \leq \boldsymbol{k}_{j+1}\}$ [5].

1) Polytopic Passive Backwards Reachable Sets: Similarly, the passive BRS (PBRS) are also polytopic, since polytopes are closed under affine transformations. They can be derived by using the above sets and letting $\mathcal{U}_i = \{\mathbf{0}\}$. If $t_j = t_f - j\Delta t$, and the state transition matrix from t_j to t_f is $\Phi(t_f, t_j)$, then the j-steps PBRS polytope is

$$\mathcal{R}_b(j; \mathcal{P}_f, \{\mathbf{0}\}, t_f) = \{\boldsymbol{x} \in \mathbb{R}^n : \ H_f \Phi(t_f, t_f - j\Delta t)\boldsymbol{x} \leq \boldsymbol{k}_f\}, \quad (8)$$

which can be computed recursively or by iterating on t_j. Note that taking their union leads the PBRS over an interval (PBRSI).

B. Ellipsoidal Passive Backwards Reachable Sets

In the case the target set is an ellipsoid $\mathcal{E}_f$, the resulting PBRS will also be ellipsoidal since ellipsoids are closed under affine transformations. The j-steps ellipsoidal passive backwards reachable set is given by

$$\mathcal{R}_b(j; \mathcal{E}_f, \{0\}, t_f) = \{\mathbf{x} \in \mathbb{R}^n : \mathbf{x}^\top \Phi(t_f, t_f - j)^\top \ P^{-1} \ \Phi(t_f, t_f - j) \ \mathbf{x} \leq 1\}. \quad (9)$$

We only use ellipsoidal sets to compute the sets for passive safety i.e. when $\mathcal{U} = \{\mathbf{0}\}$.

IV. Coasting Arcs

Minimizing the delta-v used and getting sparser control signals fundamentally requires leveraging the natural dynamics efficiently. We define a goal set, $\mathcal{G}_f$ that is near the original avoidance set $\mathcal{S}_f$. Computing the N-steps PBRSI of the goal set results in the sets of all states that naturally drift into $\mathcal{G}_f$ in N-steps or less. We denote the PBRSI of the goal set as the *coasting sets*. By construction, the avoidance and goal set are "close" to each other in $\mathbb{R}^n$. Given the dynamics of the problem, the PBRSI of $\mathcal{G}_f$ and $\mathcal{S}_f$ for each set tend to have non-empty intersections with respect to each other, which makes trying to enter the coasting sets, while avoiding the unsafe PBRSI, challenging. Figure 1 shows some of the projected PBRS coasting sets for $\mathcal{G}_f$ in blue, and projected PBRS unsafe set for $\mathcal{S}_f$ in red, where $\mathcal{G}_f$ is a polytope, and $\mathcal{S}_f$ is an ellipsoid.

The goal set is designed to constrain the final approach location and velocity. Since passive-safety is required during the coasting arc, no union over the considered failure modes is necessary. As such we use the LTV-RBRSI (4) to construct the PBRSI, and neglect (6). The PBRSI from $\mathcal{G}_f$ are given by $\mathcal{R}(N_c; \mathcal{G}_f, \{0\}, t_f)$, which defines the set of all states that enter $\mathcal{G}_f$ in at most N_c steps at the final time t_f. The goal set is defined such that its intersection with $\mathcal{S}_f$ is empty, i.e., $\mathcal{G}_f \cap \mathcal{S}_f = \emptyset$. Naturally, the states in $\mathcal{R}(N; \mathcal{G}_f, \{0\}, t_f)$ need

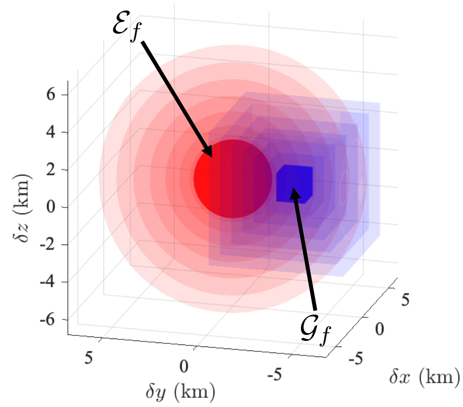

Fig. 1: Projection of the coasting sets (blue) and the passively unsafe sets (red) onto the 3D position subspace for an NRHO target.

not be passively-safe. That is, for some $\delta t > 0$, there may exist a state $\boldsymbol{x}(t) \in \mathcal{G}_f$ such that $\boldsymbol{x}(t+\delta t) \in \mathcal{S}_f$ or vice-versa, there may exist a state $\boldsymbol{x}(t) \in \mathcal{S}_f$ such that $\boldsymbol{x}(t+\delta t) \in \mathcal{G}_f$. Given the former scenario, we note that

$$\mathcal{G}_f \cap \mathcal{R}(N; \mathcal{S}_f, \{0\}, t_f) \neq \emptyset \quad (10)$$

$$\implies \mathcal{R}(N; \mathcal{G}_f, \{0\}, t_f) \cap \mathcal{R}(N; \mathcal{S}_f, \{0\}, t_f) \neq \emptyset, \quad (11)$$

where the complexity of the intersection computation will depend on the geometric properties of the sets used.

From a coasting-arc and passive safety perspective, if $\mathcal{R}(N_c; \mathcal{G}_f, \{0\}, t_f) \cap \mathcal{R}(N; \mathcal{S}_f, \{0\}, t_f) = \emptyset$, then one can drive the chaser into $\mathcal{R}(N_c; \mathcal{G}_f, \{0\}, t_f)$ without passive safety constraints. Since this is not the case for rendezvous problems, as (11) is in general non-empty, we formulate a method for the chaser spacecraft to enter the passively-safe portion of $\mathcal{R}(N_c; \mathcal{G}_f, \{0\}, t_f)$,

$$\mathcal{C} = \mathcal{R}(N_c; \mathcal{G}_f, \{0\}, t_f) \setminus \bar{\mathcal{R}}_N(\mathcal{S}_f, \{0\}), \quad (12)$$

without explicitly computing the set difference. The set $\mathcal{C}$ is the union of passively-safe coasting sets that enter $\mathcal{G}_f$ at t_f in N_c steps or less. If the approach is constrained to be passively-safe for N steps, we require $N_c \leq N$ for the resulting coasting-arc to have a safety-horizon $N\Delta t$.

Since we consider an LTV system (1), entering $\mathcal{G}_f$ is a time-depedent problem where the relative state of the chaser $\boldsymbol{x}$ has to be an element of the correct $\mathcal{R}_b(\cdot) \subset \mathcal{R}(N_c; \mathcal{G}_f, \{0\}, t_f)$ to ensure a coasting arc from an initial (or current) time t_j to a final time t_f. That is, if $t_j = t_f - j\Delta t$, and $\boldsymbol{x}(t_j) \in \mathcal{R}_b(N_c - k; \mathcal{G}_f, \{0\}, t_f)$ where $j \neq k$, there are no guarantees that $\boldsymbol{x}(t_f) \in \mathcal{G}_f$ due to the LTV nature of the system. To obtain a successful coasting arc, we specify a fixed final coasting time t_c at which we seek to enter the goal set. Given an initial maneuver time t_0, the maximum maneuver duration is thus $t_m = t_c - t_0$. The resulting maximum number of coasting steps is $N_c = \frac{t_m}{\Delta t}$, and in addition $t_c \leq t_f$ to ensure safety for the allotted time-horizon. To enforce a coasting arc, the following constraints have to be satisfied

$$\boldsymbol{x}(t_j) \in \mathcal{R}_b(N_c - j; \mathcal{G}_f, \{0\}, t_c),\ j \in \{0, \dots, N_c\}. \quad (13)$$

Since initially $\boldsymbol{x}(t_0) \notin \mathcal{R}(N_c; \mathcal{G}_f, \{0\}, t_c)$, (13) has to be implemented as soft constraint to avoid infeasibility. Once (13) is satisfied, the chaser has entered a coasting set for step j and hence it will passively coast to $\mathcal{G}_f$ in $N_c - j$ steps.

V. Rendezvous Control

For the complete entire rendezvous mission, we consider two controllers: the first one steers the spacecraft from the initial position to the final approach corridor while enforcing passive safety and exploiting coasting arcs. The second controller is engaged when the spacecraft enters the final approach corridor while enforcing abort-safety. Both controllers are implemented using MPC, where the only differences lie in the imposed constraints.

A. Optimal Control Problem

The *non-coasting* MPC policy yields a constrained trajectory that is safe while driving the chaser to approach the target. Conversely, the *coasting* MPC, appends the coasting set constraints in the initial rendezvous phase to the *non-coasting* MPC formulation. As such, the following optimal control is solved

$$\begin{aligned}
\min_{\boldsymbol{U}_t} \quad & E(\boldsymbol{x}_{N_p|t}) + \sum_{k=0}^{N_p-1} F(\boldsymbol{x}_{k|t}, \boldsymbol{u}_{k|t}, s_{k|t}) && \text{(14a)}\\
\text{s.t.} \quad & \boldsymbol{x}_{k+1|t} = A_d(t+k)\boldsymbol{x}_{k|t} + B_d(t+k)\boldsymbol{u}_{k|t} && \text{(14b)}\\
& g_t(\boldsymbol{x}_{k|t}, \boldsymbol{u}_{k|t}, s_{k|t}) \le 0 && \text{(14c)}\\
& u_{k|t} \in \mathcal{U}(t) && \text{(14d)}\\
& \boldsymbol{x}_{0|t} = \boldsymbol{x}_t && \text{(14e)}\\
& s_{k|t} \ge 0 && \text{(14f)}
\end{aligned}$$

where N_p is the prediction horizon length, usually (much) smaller than N in (5), the prediction model (14b) is (1), (14c) is the constraint ensuring safety (passive or abort) as well as a desired coasting arc. Additionally, $\mathcal{U}(t) \in \{\mathcal{U}_i\}_i$ is the input set at time t, which depends on the propulsion system condition according to (2). Since the control sequence over the horizon is $\boldsymbol{U}_t = (\boldsymbol{u}_{0|t} \dots \boldsymbol{u}_{N_p-1|t})$, the following control is applied as an input

$$\boldsymbol{u}_t = \kappa_{mpc}(\boldsymbol{x}_t) = \boldsymbol{u}^*_{0|t}, \quad (15)$$

where $\boldsymbol{U}^*_t = (\boldsymbol{u}^*_{0|t} \dots \boldsymbol{u}^*_{N_p-1|t})$ is the optimizer of (14).

B. Constraints

1) Passive-Safety: Passive safety is maintained with respect to a terminal ellipsoidal set. As such, we implement a local convexification approach that uses a tangent to an ellipsoid in the PBRSI to construct a local half-space constraint that approximates $\boldsymbol{x} \notin \bar{\mathcal{R}}(N; \mathcal{E}_f, t_f)$. Given a state $\boldsymbol{x}$ at time t, we project the state radially onto all ellipsoids $\mathcal{E}_i \in \bar{\mathcal{R}}(N; \mathcal{E}_f, t_f)$, yielding a set of points $\{\boldsymbol{x}^{s_i}\}_{i=1}^{N_s}$, where $\boldsymbol{x}^{s_i} \in \mathcal{E}_i$ and $N_s = |\bar{\mathcal{R}}_{\text{unsafe}}(N; \mathcal{S}_f)|$ is the number of sets in the LTV-PBRSI [11].

2) Abort-Safety: Similarly, we impose constraints on the state to remain outside of the abort-unsafe sets (RBRSI) (6) by computing a half-space that excludes $\bar{\mathcal{R}}_{\text{unsafe}}(\cdot)$ based on Result 1 in [5]. Specifically, a set of nearby polyhedra $\{\mathcal{P}(H_i, k_i)\}_{i=1}^{\ell} \subset \bar{\mathcal{R}}_{\text{unsafe}}(N; \mathcal{S}_f)$ are used to construct a halfspace $\mathcal{P}_h(\boldsymbol{h}, 1) = \{\boldsymbol{x} \in \mathbb{R}^n : \boldsymbol{h}^\top \boldsymbol{x} \le 1\}$ such that $\mathcal{P}_h(\boldsymbol{h}, 1) \supset \{\mathcal{P}(H_i^{\bar{\mathcal{R}}}, \boldsymbol{k}_i^{\bar{\mathcal{R}}})\}_{i=1}^{\ell}$. That is, a half-space that contains a subset of $\bar{\mathcal{R}}_{\text{unsafe}}(\cdot)$ is constructed and its complement is used to maintain abort-safety.

For both passive and abort-safety, the hyperplanes are computed based on the previously predicted state trajectory. Let $(\boldsymbol{x}_{0|t-1} \dots \boldsymbol{x}_{N_p|t-1})$ be the trajectory computed at time $t-1$, then, we compute $\boldsymbol{h}_{k|t}$ for both safety scenarios using $\boldsymbol{x}_{k+1|t-1}$ as a prediction for $\boldsymbol{x}_{k|t}$.

3) Coasting Arcs: The coasting constraints throughout the horizon are given by (13). We let $\mathcal{G}_f = \mathcal{P}(H_g, \boldsymbol{k}_g)$ be a polytope such that the PBRS are given by

$$\mathcal{R}_b(j, \mathcal{G}_f, \{\boldsymbol{0}\}, t_c) = \mathcal{P}(H_g \Phi(t_c, t_c - j\Delta t), \boldsymbol{k}_g). \quad (16)$$

Given the current time step t, the appropriate coasting set is targeted by enforcing

$$\begin{aligned}
& H_g \Phi(t_c, \tilde{t}_0)\boldsymbol{x}_{k|t} \le \gamma \boldsymbol{k}_g + \mathbb{1} s_{k|t}, \\
& \tilde{t}_0 = t_0 + (k+t)\Delta t,\ \forall k \in \{0, \dots, N_p\},
\end{aligned} \quad (17)$$

where the slack variable $s_{k|t}$ is used to avoid infeasibility since $\boldsymbol{x}(t_0) \notin \mathcal{R}(N; \mathcal{G}_f, \{\boldsymbol{0}\}, t_c)$ and the scalar $\gamma \in [0, 1)$ tightens the constraint to target the interior of the coasting set. The cost function penalty on the slack variables $s_{k|t}$ minimizes the infeasibility, which results in driving the chaser into the coasting set.

4) Line-of-sight: A LOS constraint is added to the final abort-safety phase which maintains the chaser spacecraft within a corridor that leads to an assumed docking port on the target. This constraint requires the state of the chaser to remain within a cone $A_{\text{los}}\boldsymbol{x}_{k|t} \le \boldsymbol{b}_{\text{los}}$. Additionally, the goal set is constructed to be contained within the LOS cone, i.e., $\mathcal{G}_f \subset \mathcal{P}(A_{\text{los}}, \boldsymbol{b}_{\text{los}})$, as shown in Figure 2.

5) Summary: Since the coasting-arc is useful when the chaser is far relative to the target, these coasting constraints are only used in the initial rendezvous phase where passive safety is required. Conversely, the LOS constraints are only necessary when the chaser is heading towards a docking port. Thus, for the initial approach, we can write the passively-safe path constraints, $\boldsymbol{g}_p$ as

$$\boldsymbol{g}_p(\boldsymbol{x}_{k|t}, s_{k|t}) = \begin{bmatrix} -\boldsymbol{h}_{k|t}^\top \boldsymbol{x}_{k|t} + 1 \\ H_g \Phi(t_c, k+t)\boldsymbol{x}_{k|t} - \mathbb{1} s_{k|t} - \gamma \boldsymbol{k}_g \end{bmatrix} \le \boldsymbol{0}. \quad (18)$$

When a coasting set is entered, control is switched off, so the passively-safe control policy is summarized by

$$\boldsymbol{u}_t = \begin{cases} \kappa_{mpc}(\boldsymbol{x}_t) \in \mathcal{U}, & \boldsymbol{x}_t \notin \mathcal{R}_b(N_c - t, \mathcal{G}_f, \{0\}, t_c) \\ \boldsymbol{0} \in \mathbb{R}^3, & \boldsymbol{x}_j \in \mathcal{R}_b(N_c - t, \mathcal{G}_f, \{0\}, t_c) \end{cases} \quad (19)$$

For active safety, we replace the passive safety constraints (using PBRSI) with the abort-safety constraints (using RBRSI). Additionally, the coasting constraints are exchanged for the LOS cone, yielding

$$\boldsymbol{g}_a(\boldsymbol{x}_{k|t}) = \begin{bmatrix} -\boldsymbol{h}_{k|t}^\top \boldsymbol{x}_{k|t} + 1 \\ A_{\rm los}\boldsymbol{x}_{k|t} - \boldsymbol{b}_{\rm los} \end{bmatrix} \leq \boldsymbol{0}. \tag{20}$$

C. Cost Function

In order to obtain in (14) a linear quadratic MPC, we design the stage cost and the terminal cost in (14a) as

$$F(\boldsymbol{x}, \boldsymbol{u}, s) = \boldsymbol{x}^\top Q \boldsymbol{x} + \boldsymbol{u}^\top R \boldsymbol{u} + w_s s, \tag{21a}$$
$$E(\boldsymbol{x}) = \boldsymbol{x}^\top M \boldsymbol{x}, \tag{21b}$$

where the weight matrices $Q = Q^\top \geq 0$, $R = R^\top > 0$, $M = M^\top > 0$, $w_s > 0$ are selected to achieve the desired performance. The primary objective is to approach the target affected by Q. A secondary objective is to minimize the total required propellant affected by R.

VI. Simulation Results

The simulation performs both the passive and abort-safe rendezvous mission in a phased manner. Initially, passive safety is maintained with respect to an ellipsoidal set $\mathcal{E}_f$ while a coasting set is targeted. After coasting into the goal set, abort-safety is maintained with respect to a polytopic set $\mathcal{P}_f$. The developed method is compared to a non-coasting MPC policy in terms of maneuver delta-v and input signal sparsity. The total ΔV of a maneuver is given by $\Delta V = \sum_{i=0}^{N-1} ||B_d(\cdot)\boldsymbol{u}_i|| \cdot \Delta t_{\rm MPC}$.

In the simulations, $\Delta t_{\rm MPC} = \Delta t_{\rm RBRS} = 30$s, and the nominal admissible control set $\mathcal{U}_n$, i.e., without any loss of thrust, is such that $\boldsymbol{u}_u = -\boldsymbol{u}_l = \mathbb{1} \cdot 30$N. Passive safety is maintained with respect to an ellipsoidal set where $P = \text{diag}(\begin{bmatrix} 2^2 \cdot \mathbb{1}_{1\times3} & 0.1^2 \cdot \mathbb{1}_{1\times3} \end{bmatrix}^\top)$, i.e., an ellipsoid with position and velocity of major-axes of 2km and 0.100km/s, respectively. The goal set $\mathcal{G}_f$ is a box with ±1.5km in the positions and ±5m/s in velocities. The coasting time is $t_c = 6$ hours.

The initial condition is randomly sampled such that $\boldsymbol{x}(t_0) \notin \mathcal{R}(N; \mathcal{E}_f, \{0\}, t_f)$ and $\boldsymbol{x}(t_0) \notin \mathcal{R}(N_c; \mathcal{G}_f, \{0\}, t_f)$. With reference to Figures 2-3, the initial condition is shown in red. In the former, the projection of the goal set $\mathcal{G}_f$ onto the position subspace is shown as a green polytope, while the LOS cone, which is a superset of the goal set $\mathcal{G}_f$, is shown in light blue. When coasting set constraints are used, the chaser aims to enter a nearby coasting set.

A. Lunar Gateway Rendezvous at Perilune

At perilune, the dynamics along the NRHO are the fastest and coupled in all three Cartesian directions, resulting in non-intuitive coasting trajectories. The chaser begins approximately 16km away from the target.

1) Passively-safe approach: The resulting approach trajectories are shown in Figure 2, the solution without coasting in red, and the solution with coasting arc in blue. The corresponding control signals are shown in Figures 4a-4b. For the case with coasting arc, only two input steps are required to enter a nearby coasting set. This results in an impulse-like input as shown in Figure 4a, leading the chaser into a coasting arc after two discrete-time steps.

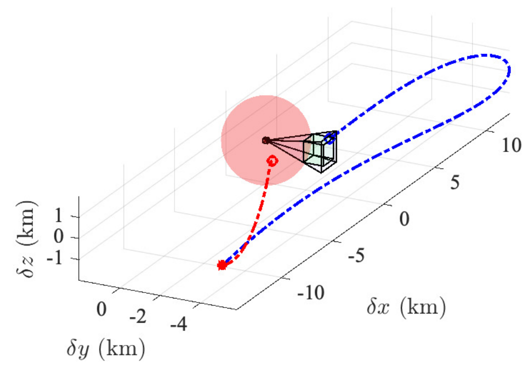

Fig. 2: In red, the MPC solution without a coasting arc while, in blue, MPC with a coasting arc. Both are passively-safe.

The resulting trajectory is almost entirely driven by the natural dynamics and the chaser enters $\mathcal{G}_f$ with an approach velocity well below the designed approach velocity limits. Moreover, Figure 3 shows samples along the controlled-arc of the maneuver, which are propagated naturally for the considered safety-horizon, to show that the chaser is indeed passively-safe. Once the chaser has entered a coasting-arc in a safe manner, the coasting-arc will also be safe, see the trajectory of Figure 3 that enters $\mathcal{G}_f$, shown in green.

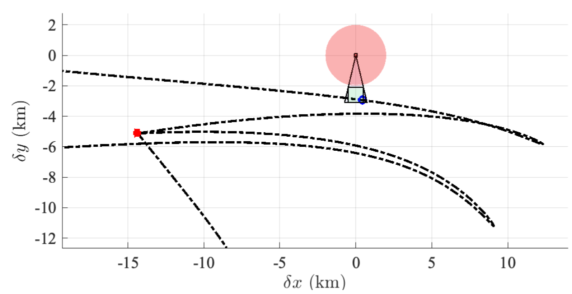

Fig. 3: Demonstration of passive safety by sampling states along the controlled portion (pre-coasting) and propagating them forward. None enter the red avoidance set.

The benefit of the design introduced here is clear as the coasting-arc safe MPC gives $\Delta V = 2.657$m/s, while the standard safe MPC approach gives $\Delta V = 9.6914$m/s, yielding a 72.5% reduction in fuel consumption. In addition, the coasting-arc solution has a control signal that is much sparser in time, which is preferable for spacecraft thruster management to reduce propulsion system failures.

For the standard MPC to obtain a trajectory similar to the one with coasting arc, an extremely large prediction-horizon N_p would have to be considered. This would come at the cost of computation as the entire QP-MPC would be much larger and the safety constraints convexification will also involve many more steps. Thus, the coasting-arc MPC that can utilize much shorter N_p seems much more practical for on-board

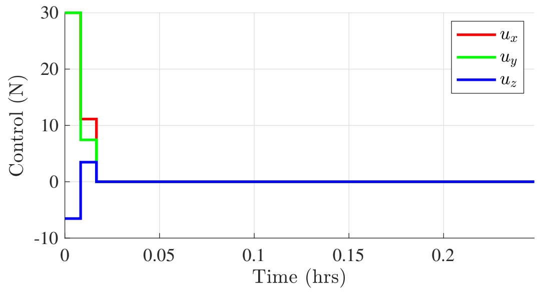

(a) Safe control signal with coasting arcs; only 0.2 hours shown out of the almost 6 hour arc. Resulting $\Delta V = 2.657$ m/s.

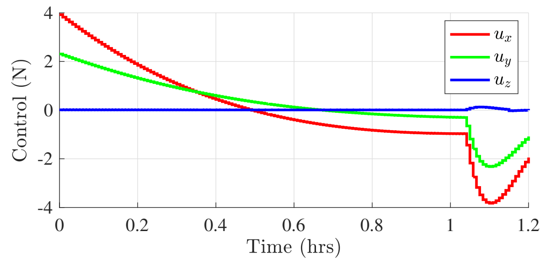

(b) Safe control signal without coasting arcs. Resulting $\Delta V = 9.6914$ m/s.

Fig. 4: Safe control histories: coasting vs. non-coasting MPC.

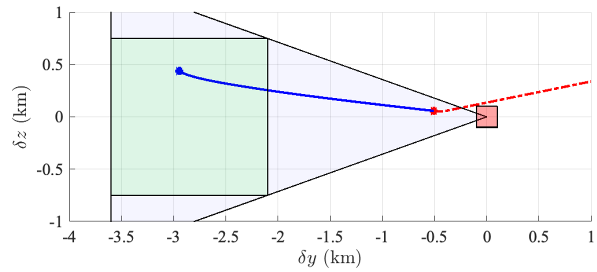

(a) Abort-safe approach toward the terminal polytope $\mathcal{P}_f$, in blue, simulated abort, in red.

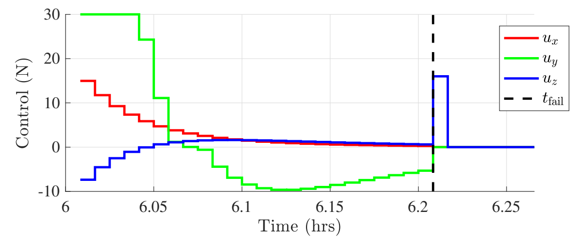

(b) Control history before and after the simulated abort at t_{fail}.

Fig. 5: Abort-safe approach, before and after abort.

use.

2) *Abort safety:* Once the spacecraft enters $\mathcal{G}_f$, the abort-safety phase is initiated. Here, the chaser has to remain outside of the RBRS, constructed with a hypothesized failure mode (additional failures can be easily included), such that in the event of a failure, a feasible abort maneuver exists. The incorporation of the LOS constraints severely limits the feasible abort maneuvers and approaches. As seen in Figure 5a, the LOS extends towards $-\delta y$. The assumed failure mode is such that $u_x = 0$, $0 \leq u_y \leq 30$N, $0 \leq u_z \leq 30$N, i.e., only positive y and z thrusts are available after a failure time t_{fail}. The chaser is able to avoid entering the RBRS while getting close to the target as seen in Figure 5a and as such, a viable abort-maneuver exists from t_{fail} onwards. The resulting control signal is shown in Figure 5b. A small impulse is applied to avoid collision.

VII. Conclusions

A safe rendezvous strategy that increasingly exploits the natural dynamics is presented. The work considers a target in a high-fidelity NRHO. A chaser spacecraft is steered into the constructed *coasting sets*, which contain the set of all states that naturally coast into a specified goal set, while maintaining passive-safety. Once the chaser is in close-proximity to the target, abort-safety is maintained. The developed coasting arc approach reduces both the amount of propellant used and the required thruster on-time, important for thruster management and thruster fault mitigation.

References

[1] U. Eren, A. Prach, B. B. Koçer, S. V. Raković, E. Kayacan, and B. Açıkmeşe, "Model predictive control in aerospace systems: Current state and opportunities," *Journal of Guidance, Control, and Dynamics*, vol. 40, no. 7, pp. 1541–1566, 2017.

[2] G. Chavers, N. Suzuki, M. Smith, L. Watson-Morgan, S. W. Clarke, W. C. Engelund, L. Aitchison, S. McEniry, L. Means, M. DeKlotz, *et al.*, "NASA's human lunar landing strategy," in *70th Int. Astronautical Congress, IAF Human Spaceflight Symposium*, 2019.

[3] W. Fehse, *Automated rendezvous and docking of spacecraft*. Cambridge university press, 2003, vol. 16.

[4] L. S. Breger and J. P. How, "Safe trajectories for autonomous rendezvous of spacecraft," *Journal of Guidance, Control, and Dynamics*, vol. 31, no. 5, pp. 1478–1489, 2008.

[5] D. Aguilar Marsillach, S. Di Cairano, and A. Weiss, "Abort-safe spacecraft rendezvous in case of partial thrust failure," in *59th IEEE Conf. Decision and Control*, 2020, to appear.

[6] F. Blanchini and S. Miani, *Set-theoretic methods in control*. Springer, 2008.

[7] J.-P. Aubin, A. M. Bayen, and P. Saint-Pierre, *Viability theory: new directions*. Springer Science & Business Media, 2011.

[8] I. M. Ross, "Space trajectory optimization and L1-optimal control problems," *Elsevier Astrodynamics Series*, vol. 1, no. 1, pp. 1–14, 2006.

[9] S. Di Cairano and I. V. Kolmanovsky, "Real-time optimization and model predictive control for aerospace and automotive applications," in *American control conference (ACC)*, 2018, pp. 2392–2409.

[10] E. N. Hartley, M. Gallieri, and J. M. Maciejowski, "Terminal spacecraft rendezvous and capture with lasso model predictive control," *Int. Journal of Control*, vol. 86, no. 11, pp. 2104–2113, 2013.

[11] D. Aguilar Marsillach, S. Di Cairano, and A. Weiss, "Fail-safe rendezvous control on elliptic orbits using reachable sets," in *American Control Conf.*, 2020, pp. 4920–4925.

[12] D. Malyuta, T. Reynolds, M. Szmuk, B. Acikmese, and M. Mesbahi, "Fast trajectory optimization via successive convexification for spacecraft rendezvous with integer constraints," in *AIAA Scitech Forum*, 2020.

[13] G. Bucchioni and M. Innocenti, "Open loop safe trajectory design for cislunar NRHO rendezvous," in *American Control Conf.*, 2020, pp. 4337–4342.

[14] J. C. Sanchez, F. Gavilan, and R. Vazquez, "Chance-constrained model predictive control for near rectilinear halo orbit spacecraft rendezvous," *Aerospace Science and Technology*, 2020.

[15] V. Muralidharan, A. Weiss, and U. V. Kalabic, "Control strategy for long-term station-keeping on near-rectilinear halo orbits," in *AIAA Scitech Forum*, 2020.